Wetlands
https://doi.org/10.1007/s13157-020-01373-7

WETLANDS RESTORATION

Unmanned Aircraft System Photogrammetry for Mapping Diverse Vegetation Species in a Heterogeneous Coastal Wetland

Sara Denka Durgan[1] · Caiyun Zhang[1] · Aaron Duecaster[1] · Francesca Fourney[2] · Hongbo Su[3]

Received: 12 March 2020 / Accepted: 1 September 2020

Abstract

Acquiring detailed information on wetland plant species is critical for monitoring wetland ecosystem restoration and management. The emerging technique of Unmanned Aircraft System (UAS) photogrammetry has immense potential for such applications. In this study, we assessed the capacity of UAS photogrammetric products for classifying and mapping a large number of wetland plant species using contemporary Object-Based Image Analysis (OBIA) and machine learning methods. Our testing results in a heterogeneous coastal wetland demonstrated the benefit of centimeter-level orthoimagery and vertical products from UAS photogrammetry for mapping 17 species compared with standard aerial photography products. We achieved an overall accuracy (OA) of 71.3% and 84.8% for mapping 17 species and 10 major species, respectively. Our study suggests that UAS photogrammetry is a valuable tool for mapping wetland species composition and distribution.

Keywords UAS · Coastal wetland · Structure from motion · Species mapping · Object-based classification

Introduction

Coastal wetlands are considered one of the most productive ecosystems; yet are under increasing threat by anthropogenic and climate stressors such as fragmentation, diversion of freshwater input, and sea level rise (Browder et al. 1994; Kirwan and Megonigal 2013). Mitigating the loss of these vital resources requires the development of efficient monitoring procedures to focus restoration efforts. Species composition is an important metric for determining the ecological integrity of a wetland ecosystem and informing management strategies (Ramsey and Jensen 1996; Lee et al. 2006; Zhao et al. 2016). Vegetation species maps not only serve as a proxy for the overall health of the ecosystem, but they also reveal information on soil conditions and water quality (Morris et al. 2002). The ability to generate this data in a timely and cost-effective manner is critical for managers to track the progress of restoration activities.

Remote sensing has been utilized for mapping wetland vegetation over the past several decades. Traditional remote sensing platforms (i.e. satellites and manned aircraft) are ideal for global and regional-scale mapping, but local-scale, fragmented, and diverse wetlands require higher spatial resolution images to capture small vegetation units (Adam et al. 2010). Unmanned Aircraft Systems (UASs) have proven promising for such applications, due to their ability to acquire hyperspatial resolution imagery on the order of centimeters (Strecha et al. 2012; Zweig et al. 2015; Lu and He 2017; Pande-Chhetri et al. 2017). Moreover, UAS missions are relatively inexpensive and easy to deploy for rapid data acquisition (Colomina and Molina 2014; Nex and Remondino 2014; Klemas 2015). These combined factors make UAS-based remote sensing an attractive technique for wetland vegetation species monitoring and assessment, but UAS research in wetlands is limited compared with the application of other platforms, as recently reviewed by Mahdianpari et al. (2020) for wetland classification using remote sensing.

A few efforts have been made to map wetland vegetation species using UAS imagery. Zweig et al. (2015) applied a UAS-derived RGB imagery for mapping plant communities in the Florida Everglades and explored the effects of the

✉ Caiyun Zhang
czhang3@fau.edu

[1] Department of Geosciences, Florida Atlantic University, 777 Glades Road, Boca Raton, FL 33431, USA

[2] Cyriacks Environmental Consulting Services, 3001 SW 15th Street, Suite B, Deerfield Beach, FL 33442, USA

[3] Department of Civil, Environmental and Geomatics Engineering, Florida Atlantic University, Boca Raton, FL 33431, USA

Published online: 18 September 2020

hyperspatial resolution of UAS imagery on vegetation classification. Marcaccio et al. (2016) examined the ability of fixed-wing and multi-rotor UASs for mapping three wetland vegetation classes and illustrated the temporal advantage of UAS data for species mapping. Pande-Chhetri et al. (2017) applied a UAS for mapping emergent aquatic plant species in the freshwater wetlands of Lake Okeechobee, Florida and explored the impact of image spatial resolution on plant classification. These studies have illustrated that UAS imagery with limited spectral resolution is advantageous for wetland vegetation mapping. However, Zweig et al. (2015) and Pande-Chhetri et al. (2017) both obtained higher accuracies when the UAS imagery was spatially down sampled for pixel-based classification. As these results contradict the common belief that higher spatial resolutions are a major advantage of UAS platforms, more work is needed to validate hyperspatial imagery for wetland vegetation mapping. In addition, while these studies successfully identified a few species or communities in their study sites, the capability of UAS for mapping many plant species (e.g., more than ten) in heterogeneous wetlands has not been examined and published.

Another advantage of UAS-based remote sensing is the ability to generate 3-dimensional (3-D) products, such as a point cloud and digital surface model (DSM), using the photogrammetric technique Structure from Motion-Multi View Stereopsis (SfM-MVS). Several studies have shown that UAS SfM-MVS can produce 3-D models of comparable, or higher, accuracy than those generated using airborne light detection and ranging (lidar) (Leberl et al. 2010; Harwin and Lucieer 2012; Kalacska et al. 2017). The inclusion of the SfM-MVS derived 3-D products has improved mapping of shrubland species (Prošek and Šímová 2019), non-submerged aquatic vegetation (Husson et al. 2017), and mangrove species (Li et al. 2017; Cao et al. 2018) compared to the application of UAS-derived orthoimagery alone. SfM-MVS allows for the generation of spectral and vertical data using the same set of images, leading to an elimination of data fusion uncertainties caused by different sources or data collected at different times. This advantage of UAS photogrammetry shows potential to improve wetland species mapping by combining simultaneously generated 3-D products and orthoimagery. Again, this fusion approach has not been applied to a high diversity wetland environment.

The main objective of this study was to map a large number of plant species found in a heterogeneous coastal wetland using UAS-derived orthoimagery and 3-D products to assist with an ongoing wetland restoration project in Biscayne Bay, Florida, USA. The specific objectives include: 1) to assess whether the centimeter-level hyperspatial orthoimagery is more valuable for fine-scale wetland species mapping than traditional manned-aircraft products (i.e. 1-ft and 1-m aerial photography); 2) to explore the benefit of UAS derived 3-D products for species mapping in wetlands compared to the application of orthoimagery alone; and 3) to discuss the advantages and challenges of UAS photogrammetry for detailed wetland mapping.

Study Site and Data Collection

Study Site

Our study site is a 7.5-acre restored coastal wetland landward of a large mangrove forest adjacent to Biscayne Bay, Florida, USA, as shown in Fig. 1. Extensive freshwater wetlands with a short hydroperiod historically dominated this area when Biscayne Bay was hydrologically connected to the Greater Everglades ecosystem (Browder et al. 1994). Presently, water management and development activities have caused saltwater intrusion, an encroachment of mangroves into upper marsh communities, habitat destruction, reduction of freshwater flow, fragmentation, and the spread of invasive species in this area. To mitigate these environmental issues, multiple agencies have partnered to restore the area through invasive species removal, controlled burns, and native species plantings (Martin 2015). In order to monitor the progress of these restoration activities, methods for obtaining frequent and accurate species maps are needed.

Data Collection

UAS Survey

We conducted a UAS survey over the study site on 26 June 2018 with a 3DR Solo quadcopter UAS and payload of four Mapir Survey 3 modified-RGB cameras to capture images in red (650 nm), green (548 nm), blue (450 nm), and NIR (850 nm) wavelengths. The cameras were connected to a Survey 3 Standard GPS receiver, which provided GPS tags in the image metadata. Three missions were conducted over the study area around noon to minimize the effect of shadows. While not examined here, it has been demonstrated that the flight configuration of the UAS mission impacts photogrammetric data quality (Dandois et al. 2015; Lu and He 2018). We designed the flight plan based on the Mapir recommendations for the Survey 3 and 3DR Solo configuration, as well as the amount of image overlap recommended by Pix4D Mapper for a densely vegetated area. Each mission was flown at an altitude of 100 m above ground level (AGL), frontal overlap and sidelap of 85%, average speed of 8 mph (3.6 m/s), and a flight time of approximately 12 min. A total of 3437 images were collected over the three flights, including images from takeoff, landing, and the radiometric calibration target, comprising the primary UAS data input referred to here as the level 0 products.

To accurately georeference UAS level 0 products to a coordinate plane, ground control points (GCPs) must be deployed during a survey. We deployed 15 GCPs and measured their geographic location with a Leica Viva GS14 GNSS Real-time Kinematic (RTK). In network mode, the RTK reported relative accuracies of 3.47 mm horizontal and 6.31 mm vertical with respect to the nearest continuously operating reference station (CORS). GCP positions were recorded in the NAD83 FL East FIPS 0901 (ft) horizontal datum and the NAVD88 (ft) vertical datum using GEOID 12A. We constructed the GCPs using 2 ft. × 2 ft. plywood boards with a black and white checkerboard pattern to contrast with the landscape. The GCPs were evenly distributed throughout the study area in open areas free of dense vegetation.

In-Situ Species Data Collection

We performed a vegetation survey from 22 to 27 June 2018 to collect reference data for the UAS species mapping procedure. This field survey was planned using a stratified random sampling scheme where the study area was divided into 20 m × 20 m grids and the centroids of each grid were calculated. At each survey location, horizontal and vertical position was measured using the RTK and dominant species, minor species, and maximum canopy height were recorded within a 1 ft. × 1 ft. transect. Elevation across the study site varied from 0.28 to 0.80 m above NAVD88. We identified species of each location with assistance from field biologists at the South Florida Water Management District (SFWMD) that manages the site. Handheld camera images and samples were also collected during the survey to aid in species identification.

The field survey identified a total of 28 species present at the study site. Here, only 17 species were considered due to limited observations of several species. The most abundant species were saltbush (*Baccharis halimifolia*), giant leather fern (*Acrostichum danaeifolium*), and ragweed (*Ambrosia artemisiifolia*). Due to difficulties with identification in the UAS imagery, sand cordgrass (*Spartina bakeri*) and muhly grass (*Muhlenbergia capillaris*) were grouped together and classified as native grasses. Muhly grass and sand cordgrass are both found in the same habitats and exhibit very similar physiological, structural, textural, and spectral properties (Gilman 2014a, b). Given the limited spectral resolution it was not possible to differentiate between these species. A total of 184 species locations were measured and recorded for this study and the number of observations per species is given in Table 1.

Methods

The methodology flowchart for wetland species mapping by combining the field survey and UAS data is provided in Fig. 2. We first processed the level 0 UAS images using the SfM-MVS photogrammetry software Pix4D Mapper Pro to produce a point cloud, orthoimagery, and a DSM. We refer to these data products as level 1 meaning they are the direct outputs of the SfM-MVS photogrammetric workflow. Radiometric correction was applied to the orthomosaic, leading to the 4.23-cm orthoimage to be used for species mapping. To conduct an object-based machine learning classification, we generated the image objects from the orthoimage using an image segmentation algorithm. Object-level image features were extracted and fused with vertical data from the DSM as additional variables for species classification. We spatially matched UAS image features with the in-situ species data to create training and

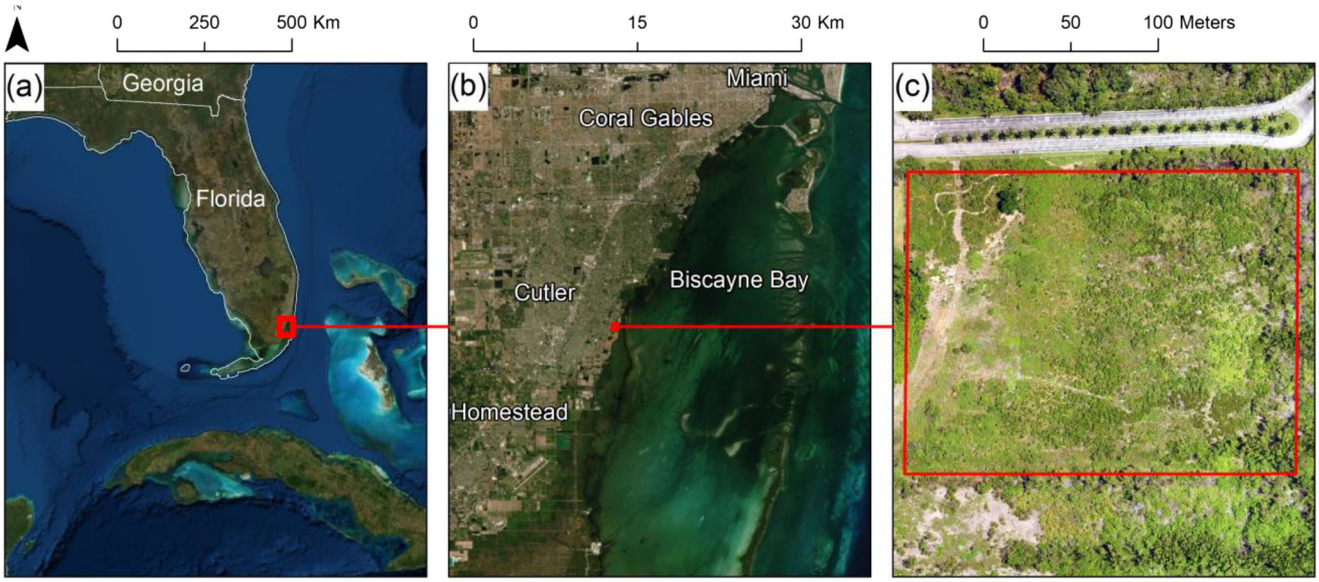

Fig. 1 Location of the study site in coastal Florida, USA (**a**); along Biscayne Bay (**b**); and shown as a natural color composite of UAS imagery (**c**)

Table 1 Number of species observations from the field survey and number of reference objects used in the classification procedure; *: a large community was found and noted in the survey

Species	# Observations	# References
Saltbush (*Baccharis halimifolia*)	30	122
Giant leather fern (*Acrostichum danaeifolium*)	19*	101
Ragweed (*Ambrosia artemisiifolia*)	16	32
Spainish needles (*Bidens alba*)	15*	71
Dog fennel (*Eupatorium capillifolium*)	15	18
Carolina willow (*Salix Carolina*)	14	68
Nealley's sprangletop (*Leptochloa nealleyi*)	13	35
Late boneset (*Eupatorium serotinum*)	13	39
Native grasses (*Spartina bakeri; Muhlenbergia capillaris*)	12	66
Napier grass (*Pennisetum purpureum*)	7	44
Saltmarsh fleabane (*Pluchea odorata*)	7	31
Mullein nightshade (*Solanum donianum*)	6	38
Vasey's grass (*Paspalum urvillei*)	5	33
Lead tree (*Leucaena leucocephala*)	4	14
Green buttonwood (*Conocarpus erectus*)	3	14
White mangrove (*Laguncularia racemose*)	3	14
Railroad vine (*Ipomoea pes-caprae*)	2*	40

testing data. We used two popular machine learning classifiers, Random Forest (RF) and Support Vector Machine (SVM), for species mapping and performed accuracy assessment using the error matrix and Kappa statistic techniques. Finally, we generated species maps and an uncertainty map by a joint analysis of the outputs from two classifiers. To evaluate the effects of spatial resolution on species identification, we spatially resampled the 4.23-cm orthomosaic to 1-ft and 1-m to simulate the traditional aerial photography products available for this area. Major steps in the UAS data processing and wetland species mapping procedure are provided in the following subsections.

UAS Level 0 Image Processing for Level 1 Product Generation

We performed SfM-MVS photogrammetry for the UAS level 0 images using Pix4D Mapper Pro software to generate level 1 products of a point cloud, orthoimage, and DSM. Before input into the photogrammetry software, we pre-processed the level 0 images through file conversion and manual filtering. We conducted SfM-MVS photogrammetry on the level 0 images using the standard steps, which includes keypoint matching, bundle block adjustment, and input of GCPs for georeferencing. More details on SfM-MVS using these steps can be found in Carrivick et al. (2016). Geometric accuracy of the UAS level 1 products was estimated by designating 8 of the 15 GCPs as checkpoints. Unlike GCPs, checkpoints are not utilized in the georeferencing process therefore provide an unbiased estimate of positional accuracy of the output data products. The average geometric accuracy in terms of root mean square error (RMSE) for the 8 checkpoints was 0.031 m in X error, 0.027 m in Y error, and 0.084 m in Z error. To ensure the highest possible positional accuracy, all 15 GCPs were utilized to generate the final level 1 datasets which are shown in Fig. 3 below.

Radiometric Calibration

Radiometric calibration was performed on each level 1 single-band orthomosaic using a camera reflectance calibration ground target and a modified empirical line method. Following the image acquisition mission, images of the reflectance calibration target were obtained from the ground. The reflectance calibration target contains 4 targets of varying brightness that have been measured using a spectrometer. The four single-band orthomosaics and the reflectance target images from each camera were loaded into the software package Mapir Camera Control to perform radiometric calibration and scaling of the pixel values relative to one another. The calibrated orthomosaics were then stacked together create the corrected 4-band orthoimage, as shown in Fig. 3a.

Image Object Generation

Object-based Image Analysis (OBIA) has proven more valuable for classifying fine spatial resolution images in wetlands than pixel-based mapping techniques (e.g., Pande-Chhetri et al. 2017; Zhang et al. 2018); therefore, we applied OBIA for species mapping in this study. Image objects were generated using the multi-resolution

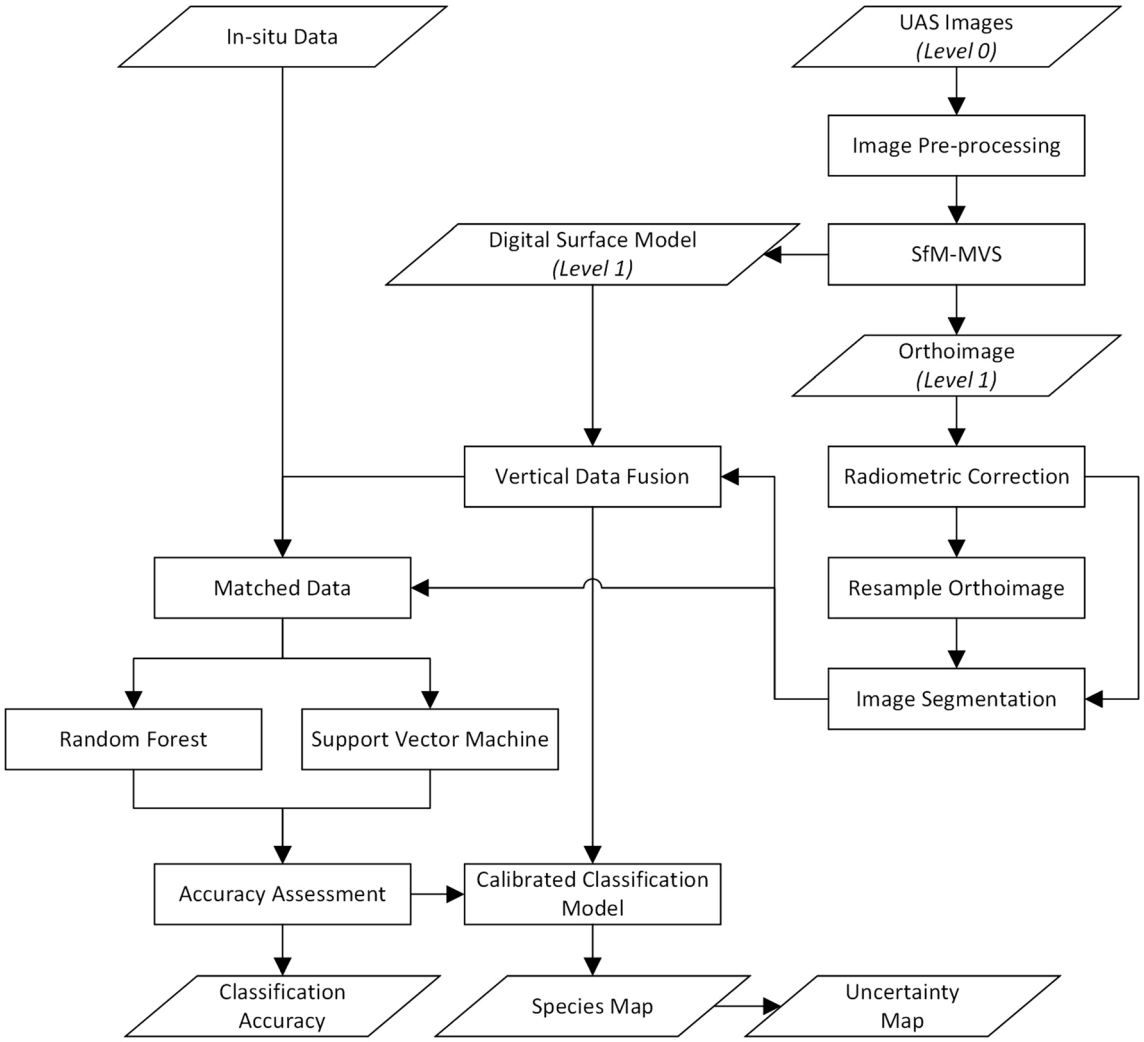

Fig. 2 The framework for the UAS data processing and classification procedure

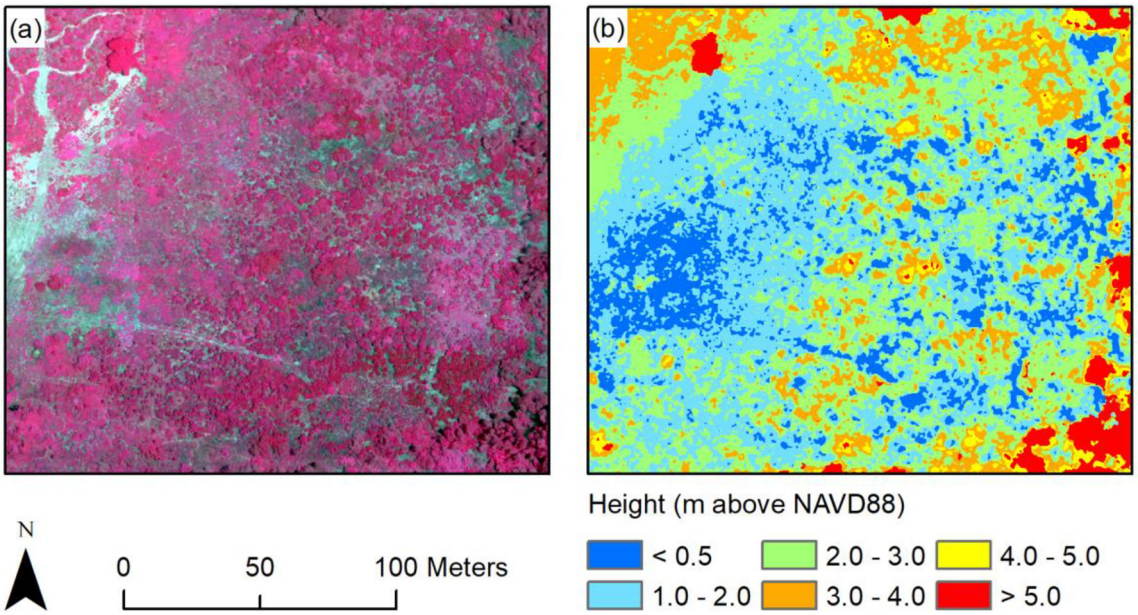

Fig. 3 Maps of the level 1 UAS products generated from SfM-MVS photogrammetry, the orthoimage displayed as a color-infrared composite (**a**), and the DSM (**b**)

segmentation algorithm in eCognition Developer 9.0 (Trimble 2014). The color/shape and smoothness/compactness parameters were set to equal weights (0.5/0.5) to favor color, texture, compact and non-compact segments equally. The scale parameter is recognized as one of the most important variables for OBIA as it determines the relative size of the image objects therefore has a significant impact on classification accuracy (Drăguț et al. 2014; Ma et al. 2015). Although automated methods for determination of the scale parameter have been explored (Johnson and Xie 2011; Drăguț et al. 2014), the most commonly used method remains the manual interpretation of how accurately image objects capture the objects of interest (Im et al. 2014). For the 4.23-cm orthomosaic, the optimal scale parameter was determined to be 250 as the largest scale for which objects captured communities of a single species. In order to make a consistent comparison with the coarser 1-ft and 1-m orthoimagery that were also segmented for object-based classification, the optimal scale parameter of these two images was determined by generating a similar number of objects as the 4.23-cm orthoimage.

Following segmentation, spatial (texture) and spectral variables of each object were extracted and combined with statistical descriptors of the DSM, leading to a fused dataset for species mapping. It should be noted that the DSM used in this study was not normalized. Unlike lidar, UAS photogrammetry does not penetrate a dense vegetation canopy to capture bare earth terrain (Kalacska et al. 2017; Meng et al. 2017). Due to the dense vegetation present at the study site, there were not enough ground features to generate a Digital Elevation Model (DEM). The vertical metrics from the DSM were variables meant to represent the relative canopy structure of each species instead of the height above ground.

Manual Interpretation of Additional Reference Samples and Data Matching

Although a total of 184 field observations were recorded during the survey, there were limited field samples for some species as shown in Table 1. Limited reference samples are likely to have a substantial effect on classification accuracy (Foody et al. 2006). As a result of the high number of plant species at the study site, additional reference samples were necessary for model training and accuracy assessment. An added benefit of UAS imagery is that the high spatial resolution facilitates visual interpretation compared with coarser-resolution imagery from traditional platforms (Chabot et al. 2018). We performed visual interpretation of the 4.23-cm UAS orthoimage and generated additional reference samples for the 17 plant species considered in the study. This interpretation was further aided by notation from the field survey detailing the presence of large communities of a single species. In total we acquired 780 reference objects and spatially matched them with the fused dataset for classifier calibration and validation. The final number of reference objects for each species is shown in Table 1. The number of reference objects remained the same across the three orthoimage datasets with different resolutions.

Classification Model Development and Final Vegetation Mapping

We selected two popular machine learning classifiers for species mapping: RF and SVM, which have been shown to perform comparatively well in wetland vegetation classification applications (Zhang et al. 2016, 2018). They have also proven successful for vegetation classification using UAS imagery (Feng et al. 2015; Lu and He 2017; Pande-Chhetri et al. 2017). RF is a machine learning classifier combining an ensemble of decision-trees (Breiman 2001). It is robust to parameter settings, small training samples, and uncertain data quality (Maxwell et al. 2018). SVM is a supervised classifier that aims to find the optimal boundary or hyperplane that can separate classes based on the training samples (Vapnik 1995). SVM is less sensitive to training sample size, however can be sensitive to uncertain data quality (Foody and Mathur 2004; Foody et al. 2006). Implementation and parameter tuning for RF and SVM was carried out in the free statistical software tool R (https://www.r-project.org/). Specifically, the caret package was used within R, which provides functions for machine learning classification and regression (Kuhn et al. 2016). If a species classification model was acceptable, we performed object-based species mapping over the entire study domain. We applied a two-step procedure for final species mapping: 1) a classification of the study site into bare ground, vegetation, and GCPs using the RF classifier; and 2) mapping species over the vegetated area using a calibrated species classification model.

Accuracy Assessment

We applied the *k*-fold cross validation technique to validate the classification (Anguita et al. 2012). *k*-fold cross validation separates the dataset into *k* subsets (i.e. folds) of approximately equal size, and then selects subsets to train and others to test model performance (Kohavi 1995). This calculation is performed iteratively in order to cross-validate the training and testing folds and calculate accuracy across all reference samples. The variable *k* was set to 5 in this study, which is a commonly used value in published literature. The *k*-fold cross procedure was used to generate error matrices and resulting accuracy metrics of overall accuracy (OA), kappa coefficient, user's

accuracy (UA), and producer's accuracy (PA), to evaluate the performance of the classifications. The classification accuracy metrics presented here are the average across all folds. Finally, McNemar's chi-squared tests were applied to evaluate whether there was a significant difference between two classifications (Foody 2004).

Results and Discussion

Effects of UAS Orthoimage Spatial Resolution on Species Classification

To evaluate the impact of UAS orthoimage spatial resolution on classification of all 17 species considered in the study, we designed three experiments using the 4.23-cm, 1 ft, and 1-m orthoimagery. The classification accuracy results are displayed in Table 2. The 4.23-cm finest resolution imagery achieved the highest accuracy among three experiments. SVM produced an OA of 68.7% and kappa coefficient of 0.66; and RF generated an OA of 65.0% and kappa coefficient of 0.62. Accuracy decreased with the decreasing image spatial resolution for both classifiers. The findings from these three experiments demonstrate that the hyperspatial resolution of UAS imagery can increase classification accuracy for wetland vegetation mapping. Zweig et al. (2015) and Pande-Chhetri et al. (2017) both found that for pixel-based assessments the hyperspatial resolution UAS orthoimagery was too complex and noisy for vegetation community and species classifications, respectively. Our results agree with the finding in Pande-Chhetri et al. (2017) that OBIA is advantageous for UAS-based species mapping, but we demonstrate that the hyperspatial resolution imagery generates more detailed variables to increase species separability.

For a wetland with this level of species diversity, UAS photogrammetric products are promising for producing more detailed species maps compared with traditional aerial photography. In the U.S., the National Agriculture Imagery Program (NAIP) collects 1-m aerial photography with 3 RGB or 4 bands (Red, Green, Blue, and Near Infrared) at a 3-year cycle since 2009. The program produces image products either as Digital Ortho Quarter Quad tiles (DOQQs) or as Compressed County Mosaics, which are publicly available for mapping applications. We found that the 1-m resolution orthoimage performed poorly as input for species classification, thus UAS surveys provide a viable alternative for data acquisition in diverse, complex wetlands compared with NAIP imagery. Local sources of aerial photography, such as U.S. county or state governments, sometimes capture higher resolution images (~1 ft) of their jurisdiction for public use. While an improvement over 1-m resolution, we show that 1-ft resolution imagery produced a low classification accuracy for this heterogeneous wetland site. Furthermore, the temporal availability of these datasets is limited due to a high cost of acquisition. Imagery with increased spectral resolution, such as hyperspectral data, is ideal for improved species classification, yet also remains cost prohibitive.

Table 2 Classification accuracies from 4.23-cm, 1-ft, and 1-m UAS 4-band orthoimagery using SVM and RF classifiers for all 17 species

Resolution	OA (%)		Kappa Value	
	SVM	RF	SVM	RF
4.23 cm	68.7	65.0	0.66	0.62
1 ft	59.9	61.9	0.56	0.58
1 m	53.0	48.9	0.48	0.44

Impact of Vertical Variables from the DSM on Species Classification

We examined the impact of vertical variables on species classification by designing 8 experiments. Experiments 1–4 were conducted for all 17 species, referred to as all species, to test whether adding vertical variables increased accuracy for both RF and SVM. Several species performed poorly in the classification procedure due to limited samples, thus we conducted Experiments 5–8 by considering the 10 major species only, referred to as major species. For all 8 experiments, only the 4.23-cm orthoimagery was tested. The performance of these experiments is provided in Table 3. Across all experiments, including vertical variables improved the classification compared to the application of orthoimagery alone. The highest accuracies were achieved by SVM for both all species (OA: 71.3%, Kappa: 0.69) and major species (OA: 84.8%, Kappa: 0.83) classifications. The improvement resulting from fusing the orthoimage with the DSM product was statistically significant based on McNemar test results. The accuracy was further improved when the classification was limited to major species identification, suggesting that adding more species can increase confusion between species in the classification, which agrees with the findings in Zhang and Xie (2013) who classified a large number of wetland plant species using hyperspectral data. SVM and RF had a comparable performance showing no statistically significant difference when the vertical variables were included in the classification.

To examine the effects of vertical variables on species identification, we calculated per-species accuracies for Experiments 1–4, as shown in Table 4. The addition of the DSM product increased classification accuracy for 15 species using RF and 12 species using SVM. Across both classifiers, Spanish needles, mullein nightshade, napier grass, and railroad vine appeared to benefit most from the inclusion of the vertical variables. With RF, all species per-class accuracies

Table 3 Classification accuracies of the different experiments; *: statistical significance (p value <0.05) for McNemar's chi-squared test

Experiment	Classification	DSM	Classifier	OA (%)	Kappa Value	χ^2 (McNemar's)
1	All Species	No	RF	65.0	0.62	6.84 (1/3)*
2	All Species	Yes	RF	70.6	0.68	18.62 (1/2)*
3	All Species	No	SVM	68.7	0.66	3.85 (3/4)*
4	All Species	Yes	SVM	71.3	0.69	0.21 (2/4)
5	Major Species	No	RF	81.3	0.79	0.04 (5/7)
6	Major Species	Yes	RF	84.1	0.82	4.59 (5/6)*
7	Major Species	No	SVM	81.7	0.79	5.55 (7/8)*
8	Major Species	Yes	SVM	84.8	0.83	0.24 (6/8)

increased except lead tree and green buttonwood, which remained at 0% accuracy, suggesting application of UAS products failed for classification of these two species. For the SVM classification, addition of the vertical variables increased the misclassification rate for several species including late boneset, saltmarsh fleabane, lead tree, green buttonwood, and white mangrove. The most dramatic change occurred for saltmarsh fleabane where the UA decreased from 82.8%–66.7%. Including the vertical variables increased the misclassification of saltmarsh fleabane with nealley's sprangletop and ragweed demonstrating that these species have similar vertical canopy structures. Overall, inclusion of the vertical variables proved more impactful for improving classification accuracy using the RF classifier as opposed to SVM.

The benefits from the vertical variables for classification agrees with the findings in similar studies (Husson et al. 2017; Li et al. 2017; Cao et al. 2018; Prošek and Šímová 2019). As previously stated, the vertical variables used in this study were calculated using the level 1 DSM and therefore were absolute height above NAVD88. As the study area was densely vegetated, we were not able to generate an accurate DEM and subsequent canopy height model (CHM), which may improve the species mapping procedure. Moreover, we did not perform any data correction on the level 1 DSM meaning it likely contained a fair amount of noise and error. As applications in UAS photogrammetry grow, tools and methods for UAS-derived photogrammetric point cloud filtering, classification, and interpolation are emerging. For example, LAStools and CloudCompare, well-known open-source software for processing lidar datasets, have recently developed functionality for processing photogrammetric point clouds. Future studies are needed to examine the applicability of these methods to

Table 4 Per-class accuracies calculated as producer's accuracy (PA, %) and user's accuracy (UA, %) for all 17 species classification; bolded values indicate increasing accuracy when vertical variables are included

Species	Experiments for All Species Classification							
	1		2		3		4	
	PA	UA	PA	UA	PA	UA	PA	UA
Saltbush	82.8	76.5	**85.2**	75.4	86.9	77.4	84.4	**81.7**
Giant leather fern	89.1	82.6	**92.1**	81.6	96.0	84.3	93.1	**87.9**
Ragweed	53.1	48.6	**59.4**	**61.3**	62.5	55.6	62.5	**60.6**
Spanish needles	81.7	70.7	**88.7**	**76.8**	80.3	75.0	**91.5**	**77.4**
Dog fennel	16.7	27.3	**27.8**	**45.5**	22.2	40.0	**27.8**	27.8
Carolina willow	63.2	62.3	**66.2**	**64.3**	63.2	55.3	**69.1**	**58.8**
Nealley's sprangletop	45.7	50.0	45.7	**51.6**	48.6	58.1	48.6	**63.0**
Late boneset	20.5	22.9	**28.2**	**37.9**	35.9	37.8	28.1	29.7
Native grasses	77.3	66.2	**86.4**	**74.0**	80.3	72.6	80.3	**76.8**
Napier grass	52.3	51.1	**56.8**	**59.5**	50.0	51.2	**54.5**	**58.5**
Saltmarsh fleabane	67.7	56.8	**77.4**	**66.7**	74.2	82.8	71.0	66.7
Mullein nightshade	63.2	61.5	**76.3**	**72.5**	57.9	67.6	**73.7**	**73.7**
Vasey's grass	66.7	68.8	**69.7**	65.7	69.7	74.2	**81.8**	**81.8**
Lead tree	7.1	0.0	7.1	0.0	7.1	50.0	7.1	50.0
Green buttonwood	0.0	0.0	0.0	0.0	0.0	0.0	0.0	0.0
White mangrove	14.3	33.3	14.3	**100.0**	28.6	57.1	28.6	40.0
Railroad vine	70.0	71.8	**85.0**	**82.9**	75.0	83.3	**87.5**	**92.1**

improve photogrammetric data quality for densely vegetated wetlands as well as the downstream impact on species classification accuracy.

Object-Based Species Mapping and Spatial Uncertainty Analysis

Based on the above experimental analysis, fusing the level 1 UAS 4.23-cm orthoimagery with the simultaneously generated DSM showed best performance for wetland species classification. We thus generated species maps using the fused dataset, as shown in Fig. 4. Because bare ground and GCPs were also present over the study site, we first delineated the vegetated area by using the RF classifier to classify the study site into bare ground, GCPs, and vegetation and achieved an OA of 99.7% and Kappa value of 0.99. We then mapped the plant species over the vegetated areas using both RF and SVM classifiers. The map showed a high spatial heterogeneity of plant species over the study area. The western part is dominated by Spanish needles and leather fern is mainly found in the southeast part.

RF and SVM had a comparable accuracy in terms of OA and Kappa statistics and they generally produced a similar species distribution pattern. While SVM achieved a slightly higher OA, RF is an easier algorithm to implement because there are only two parameters to tune while SVM requires the choice of a kernel each needing different parameters. It was difficult to discriminate the difference between the two classified maps in Fig. 4. Therefore, following Zhang et al. (2016), we created an uncertainty map displaying the spatial agreement/disagreement between the RF and SVM classifications, as shown in Fig. 5. For the vegetated areas, 62.1% of the area showed agreement (green) between the two classifiers and 37.9% had no agreement (red). While RF and SVM achieved similar classification accuracies for the all species classification, the uncertainty map displays a fair amount of disagreement over the study area. As expected, species that performed well in the classification procedure had the highest rates of agreement while the minor species showed poor agreement between the two classifiers. The uncertainty map displays the difficulty of the mapping procedure to distinguish between such a large number of species. Despite these

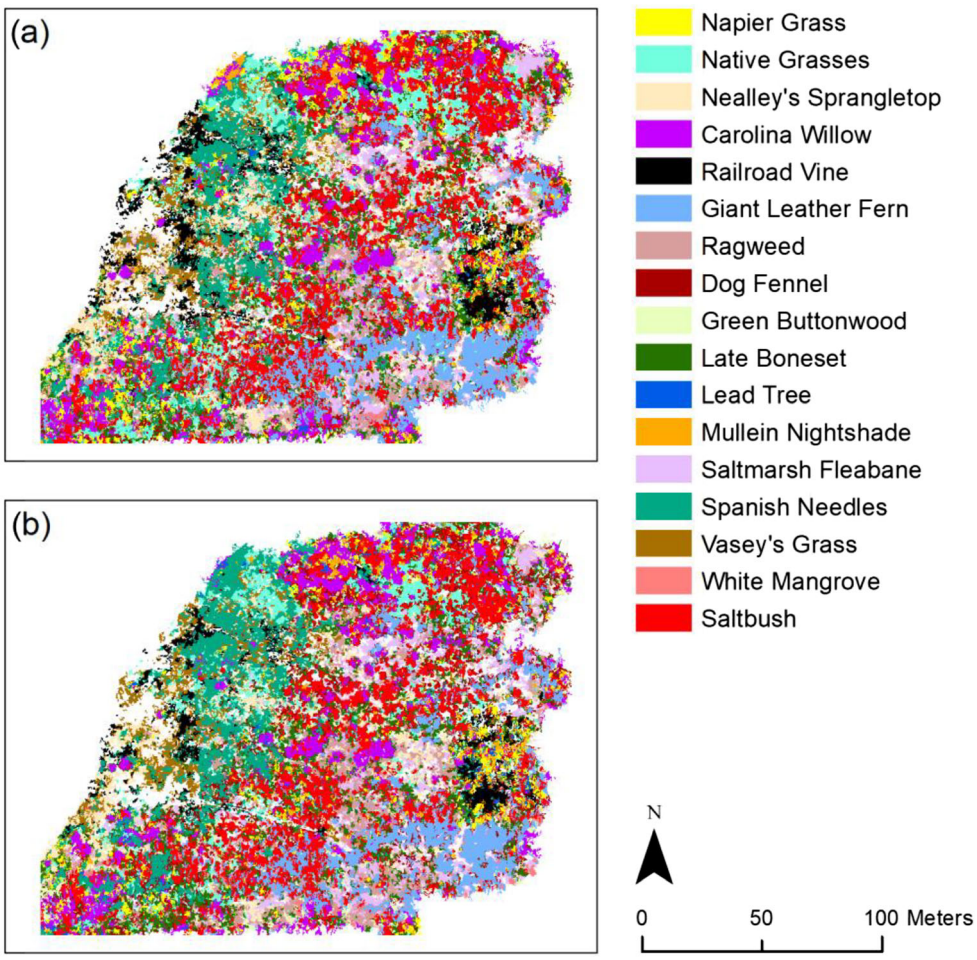

Fig. 4 Classified species maps from RF (**a**), and SVM (**b**)

areas of disagreement, the estimated species composition of the study area remained similar between the two classifiers demonstrating that UAS-based vegetation mapping is beneficial for calculating this ecological metric (results are not shown). In addition, the uncertainty map has the added benefit of directing managers towards areas where verification is needed, aiding in future surveys. For example, areas with a disagreement overlaid on the UAS orthoimage in Fig. 5b showed the challenging areas for classification, where more reference data should be collected to minimize the omission or commission errors in the classification.

Implications of UAS Species Mapping for Wetland Restoration and Management

The developed mapping procedure was successful in delineating the spatial distribution of numerous vegetation species in this restored wetland site. Many of these species are considered wetland indicator species from the 2012 National Wetland Plant List for the U.S.; therefore, the species mapping procedure can aid with federal wetland delineations and restoration (U.S. Army Corps of Engineers 2018). Several key species performed very well in the classification including saltbush (*Baccharis halimifolia*), Spanish needles (*Bidens alba*), giant leather fern (*Acrostichum danaeifolium*), and railroad vine (*Ipomoea pes-caprae*). These key species serve important roles in the overall health of wetland ecosystems. Saltbush provides nectar to numerous butterfly species, including the monarch butterfly (*Danus plexippus*), which is currently under review for inclusion in the U.S. Endangered Species Act (ESA) due to declining populations (UF IFAS 2016; U.S. Fish and Wildlife Service 2018). Spanish needles are common throughout Florida and are known to establish in disturbed areas as they can thrive within a broad range of environmental conditions (Ramirez et al. 2012). Leather ferns (*Acrostichum spp.*) are closely associated with mangrove understory vegetation worldwide and are beneficial for the mangrove forest ecosystem (Sharpe 2010; Tomlinson 2016). Finally, railroad vine is a critical species for erosion control and has been widely utilized for dune stabilization in the U.S. (Chau and Chu 2017). The ability to identify and track species distribution changes using UAS photogrammetry can provide managers with information necessary for evaluating restoration success, site maintenance, and species control for wetland environments.

The mapping procedure had mixed success classifying the invasive species present at the site which includes vasey's grass (*Paspalum urvillei*), nealley's sprangletop (*Leptochloa nealleyi*), and napier grass (*Pennisetum purpureum*). Vasey's grass had a high per-class accuracy using the SVM classifier while RF showed lower accuracy classifying this species. Nealley's sprangletop and napier grass both had low per-class accuracies in the all species classification, therefore were not considered in the major species classification. These three species are weedy grasses that are well-known invasives found throughout Florida and the Everglades, commonly in disturbed or agricultural areas. Invasive species negatively impact biodiversity, fundamental

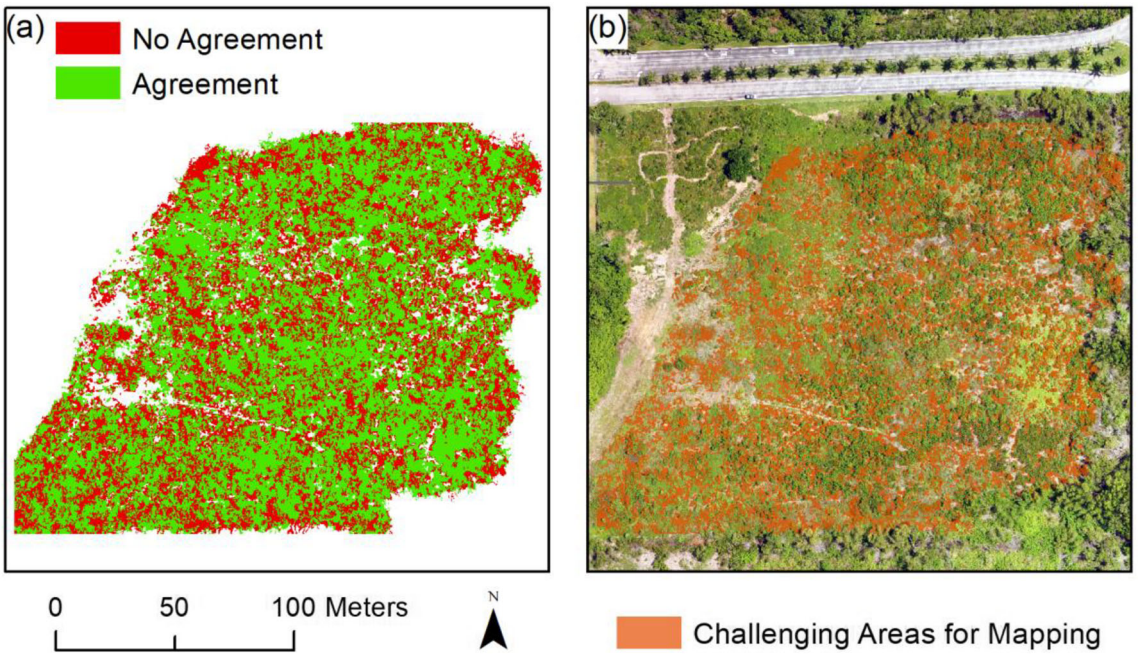

Fig. 5 The uncertainty map showing the spatial agreement between RF and SVM classifications (**a**); and identified challenging areas overlaid on the true-color orthoimage of the study area (**b**)

ecosystem processes, native plant community structure, and can amplify native plant extinction (Wilcove et al. 1998; Pimentel et al. 2000). While this mapping procedure was less successful in capturing the spatial extent of these species compared to the native ones, the species maps showed general agreement on the spatial location of the larger invasive communities. For further application of this method, we recommend investigation into variables that can improve the classification of these invasive species due to their importance in evaluating restoration efforts.

Advantages and Challenges of UAS Photogrammetry for Wetland Species Mapping

Our study demonstrates that UAS photogrammetry is a powerful tool for vegetation species mapping in coastal wetland environments. The overall advantage of this tool is that it provides wetland managers a more efficient means to track restoration progress compared to traditional field surveys, which are labor-intensive and difficult in these ecosystems (Gallant 2015). In order to implement this procedure, an initial field survey is required to train and test the classification model then repeated UAS surveys can be conducted to track species cover over time. The UAS used in this study was a consumer-grade instrument that was low-cost, easy to operate, and small for easy transport to the field. The UAS surveys over the 7-acre study area took less than 1 hour to complete compared to the field survey which required five days of work. Another field component for the UAS survey was the GCP deployment that required the use of survey-grade GPS equipment to generate high accuracy positional datasets. Survey-grade GPS equipment is often the instrument necessary for UAS surveys, but UASs with onboard RTK and post-processed kinematic (PPK) capabilities are becoming increasingly available (Obanawa et al. 2019; Peppa et al. 2019). Alternatively, a manager has the option of installing permanent targets over the area or using image-to-image registration for repeated surveys to reduce the need for GCPs.

Despite the benefits of UAS surveying for reducing costs, time, and labor in the field, there are several limitations that must be considered for the application of this method. Legal constraints such as airspace designations, licensing, and permits affect when and where UAS surveys can take place (Jeziorska 2019). In the U.S., UAS pilots need permission from the Federal Aviation Administration (FAA) to operate in controlled airspace which takes time to obtain and is not always granted. However, the recent development of the Low Altitude Authorization and Notification Capability (LAANC) has facilitated the process of obtaining airspace authorizations from the FAA (Federal Aviation Administration 2019). We chose this study site not only because it is a critical area for wetland restoration but also because it is located in a narrow strip of uncontrolled airspace, which reduced regulatory barriers for planning the survey. Dense vegetation cover is another issue using this technique for species mapping when vertical products are included, as UAS photogrammetry cannot penetrate vegetation to accurately capture terrain. While we show that vertical variables from a level 1 DSM can improve species classification, additional variables from a DEM or CHM may increase accuracy further. UAS flight configuration and post-mission data processing also present major challenges for applying UAS photogrammetry for species mapping. Our pilot studies show that flying altitude, image overlap, and lightning conditions can largely impact UAS product quality, which will inevitably impact species mapping applications. In our study, we found that 100 m altitude was sufficient for delineation of several species included in the classification; yet for certain species that establish in smaller communities, such as dog fennel, a lower flight altitude may have improved the classification. Similarly, post-mission data processing such as level 1 data generation can also impact the data quality. Understanding these effects is essential before acquiring UAS data in the field and applying photogrammetry for species mapping. Finally, UAS image processing requires high technical expertise in photogrammetry software, which can be expensive depending on the workflow requirements (Jeziorska 2019). The computational cost of UAS photogrammetry is also high as the level 0 images are often of large file size and processing can take several days (Manfreda et al. 2018). In our study, we utilized several software packages in the methodology to produce the final species map and future work in this space should consider developing a more streamlined workflow.

Conclusions

This study demonstrated that UAS photogrammetry with limited spectral resolution is a viable option for mapping a large number of plant species in a heterogeneous coastal wetland. The data acquisition and processing procedures including SfM-MVS, OBIA, and machine learning classification can inform future wetland management strategies for generating species maps of appropriate temporal and spatial scales using UAS products. Our results demonstrated that centimeter-level hyperspatial UAS imagery increases species classification accuracy compared with traditional 1-ft and 1-m aerial photography. We also found that including vertical variables from the level 1 DSM improved species classification. These findings suggest that UAS photogrammetry is beneficial for efficient monitoring of wetland restoration. Although encouraging results were achieved for our testing site, additional research is needed in other environments or areas with different species compositions to further assess the capacity of UAS for detailed vegetation mapping. We are currently working with local agencies to test this technique for plant mapping in freshwater wetlands. We hope the promising results obtained in

this study can stimulate further UAS research and applications in wetland environments.

Acknowledgements This project was supported by the National Aeronautics & Space Administration (NASA) through the University of Central Florida's NASA Florida Space Grant Consortium.

References

Adam E, Mutanga O, Rugege D (2010) Multispectral and hyperspectral remote sensing for identification and mapping of wetland vegetation: a review. Wetlands Ecology and Management 18(3):281–296. https://doi.org/10.1007/s11273-009-9169-z

Anguita D, Ghelardoni L, Ghio A, Oneto L, Ridella S (2012) The 'k' in k-fold cross validation. In ESANN 2012 Proceedings, European Symposium on Artificial Neural Networks, Computational Intelligence and Machine Learing, Burges, Belgium

Breiman L (2001) Random forests. Machine Learning 45(1):5–32. https://doi.org/10.1023/A:1010933404324

Browder JA, Gleason PJ, Swift DR (1994) Periphyton in the Everglades: spatial variation, environmental correlates, and ecological implications. In: Ogden JC, Davis S (eds) Everglades: the ecosystem and its restoration. St. Lucie Press, Boca Raton, pp 357–378. https://doi.org/10.1201/9781466571754

Cao J, Leng W, Liu K, Liu L, He Z, Zhu Y (2018) Object-based mangrove species classification using unmanned aerial vehicle hyperspectral images and digital surface models. Remote Sensing 10(1):89. https://doi.org/10.3390/rs10010089

Carrivick JL, Smith MW, Quincey DJ (2016) Structure from motion in the geosciences. Wiley, (Chapter 3), Chichester. https://doi.org/10.1002/9781118895818

Chabot D, Dillon C, Shemrock A, Weissflog N, Sager EPS (2018) An object-based image analysis workflow for monitoring shallow-water aquatic vegetation in multispectral drone imagery. ISPRS International Journal of Geo-Information 7(8):294. https://doi.org/10.3390/ijgi7080294

Chau NL, Chu LM (2017) Fern cover and the importance of plant traits in reducing erosion on steep soil slopes. CATENA 151:98–106. https://doi.org/10.1016/j.catena.2016.12.016

Colomina I, Molina P (2014) Unmanned aerial systems for photogrammetry and remote sensing: a review. ISPRS Journal of Photogrammetry and Remote Sensing 92:79–97. https://doi.org/10.1016/j.isprsjprs.2014.02.013

Dandois JP, Olano M, Ellis EC (2015) Optimal altitude, overlap, and weather conditions for computer vision UAV estimates of forest structure. Remote Sensing 7:13895–13920. https://doi.org/10.3390/rs71013895

Drăguț L, Csillik O, Eisank C, Tiede D (2014) Automated parameterisation for multi-scale image segmentation on multiple layers. ISPRS Journal of Photogrammetry and Remote Sensing 88:119–127. https://doi.org/10.1016/j.isprsjprs.2013.11.018

Federal Aviation Administration. UAS data exchange (LAANC) (2019) https://www.faa.gov/uas/programs_partnerships/data_exchange/ Accessed 20 Feb 2020

Feng Q, Liu J, Gong J (2015) UAV remote sensing for urban vegetation mapping using random forest and texture analysis. Remote Sensing 7(1):1074–1094. https://doi.org/10.3390/rs70101074

Foody GM (2004) Thematic map comparison. Photogrammetric Engineering & Remote Sensing 5:627–633. https://doi.org/10.14358/PERS.70.5.627

Foody GM, Mathur A (2004) Toward intelligent training of supervised image classifications: directing training data acquisition for SVM classification. Remote Sensing of Environment 93(1):107–117. https://doi.org/10.1016/j.rse.2004.06.017

Foody GM, Mathur A, Sanchez-Hernandez C, Boyd DS (2006) Training set size requirements for the classification of a specific class. Remote Sensing of Environment 104(1):1–14. https://doi.org/10.1016/j.rse.2006.03.004

Gallant AL (2015) The challenges of remote monitoring of wetlands. Remote Sensing 7(8):10938–10950. https://doi.org/10.3390/rs70810938

Gilman EF (2014a) Muhlenbergia capillaris Muhly Grass. UF IFAS. https://edis.ifas.ufl.edu/fp415 Accessed 12 Jul 2020

Gilman EF (2014b) Spartina bakeri Marsh Grass, Sand Cordgrass. UF IFAS. https://edis.ifas.ufl.edu/fp554 Accessed 12 Jul 2020

Harwin S, Lucieer A (2012) Assessing the accuracy of georeferenced point clouds produced via multi-view stereopsis from unmanned aerial vehicle (UAV) imagery. Remote Sensing 4(6):1573–1599. https://doi.org/10.3390/rs4061573

Husson E, Reese H, Ecke F (2017) Combining spectral data and a DSM from UAS-images for improved classification of non-submerged aquatic vegetation. Remote Sensing 9(3):247. https://doi.org/10.3390/rs9030247

Im J, Quackenbush LJ, Li M, Fang F (2014) Optimum scale in object-based image analysis. In: Weng Q (ed) Scale issues in remote sensing. Wiley, Hoboken, pp 197–214. https://doi.org/10.1002/9781118801628.ch10

Jeziorska J (2019) UAS for wetland mapping and hydrological modeling. Remote Sensing 11(17):1997. https://doi.org/10.3390/rs11171997

Johnson B, Xie Z (2011) Unsupervised image segmentation evaluation and refinement using a multi-scale approach. ISPRS Journal of Photogrammetry and Remote Sensing 66(4):473–483. https://doi.org/10.1016/j.isprsjprs.2011.02.006

Kalacska M, Chmura GL, Lucanus O, Bérubé D, Arroyo-Mora JP (2017) Structure from motion will revolutionize analyses of tidal wetland landscapes. Remote Sensing of Environment 199:14–24. https://doi.org/10.1016/j.rse.2017.06.023

Kirwan ML, Megonigal JP (2013) Tidal wetland stability in the face of human impacts and sea-level-rise. Nature 504(7478):53–60. https://doi.org/10.1038/nature12856

Klemas V (2015) Coastal and environmental remote sensing from unmanned aerial vehicles: an overview. Journal of Coastal Research 31(5):1260–1267. https://doi.org/10.2112/JCOASTRES-D-15-00005.1

Kohavi R (1995) A study of cross-validation and bootstrap for accuracy estimation and model selection. In: Mellish CS (ed) Proceedings of the fourteenth international joint conference on artificial intelligence. Morgan Kaufmann, San Francisco, pp 1137–1143

Kuhn M, Wing J, Weston S, Williams A, Keefer C, Engelhardt A (2016) Caret: Classification and regression training. https://CRAN.R-project.org/package=caret Accessed 20 Jan 2020

Leberl F, Irschara A, Pock T, Meixner P, Gruber M, Scholz S, Wiechert A (2010) Point clouds. Photogrammetric Engineering & Remote Sensing 76(10):1123–1134. https://doi.org/10.14358/PERS.76.10.1123

Lee SY, Dunn RJK, Young RA, Connolly RM, Dale PER, Dehayr R, Lemckert CJ, Mckinnon S, Powell B, Teasdale PR, Welsh DT (2006) Impact of urbanization on coastal wetland structure and function. Austral Ecology 31(2):149–163. https://doi.org/10.1111/j.1442-9993.2006.01581.x

Li QS, Wong FKK, Fung T (2017) Assessing the utility of UAV-borne hyperspectral image and photogrammetry derived 3D data for wetland species distribution quick mapping. In The International Archives of the Photogrammetry, Remote Sensing and Spatial Information Sciences, XLII-2/W6, 209–215. International Conference on Unmanned Aerial Vehicles in Geomatics, Bonn

Lu B, He Y (2017) Species classification using unmanned aerial vehicle (UAV)-acquired high spatial resolution imagery in a heterogeneous

grassland. ISPRS Journal of Photogrammetry and Remote Sensing 128:73–85. https://doi.org/10.1016/j.isprsjprs.2017.03.011

Lu B, He Y (2018) Optimal spatial resolution of unmanned aerial vehicle (UAV)-acquired imagery for species classification in a heterogeneous grassland ecosystem. GIScience & Remote Sensing 55(2): 205–220. https://doi.org/10.1080/15481603.2017.1408930

Ma L, Cheng L, Li M, Liu Y, Ma X (2015) Training set size, scale, and features in geographic object-based image analysis of very high resolution unmanned aerial vehicle imagery. ISPRS Journal of Photogrammetry and Remote Sensing 102:14–27. https://doi.org/10.1016/j.isprsjprs.2014.12.026

Mahdianpari M, Granger JE, Mohammadimanesh F, Salehi B, Brisco B, Homayouni S, Gill E, Huberty B, Lang M (2020) Meta-analysis of wetland classification using remote sensing: a systematic review of a 40-year trend in North America. Remote Sensing 12(11):1882. https://doi.org/10.3390/rs12111882

Manfreda S, McCabe MF, Miller PE, Lucas R, Pajuelo Madrigal V, Mallinis G, Ben Dor E, Helman D, Estes L, Ciraolo G, Müllerová J, Tauro F, De Lima MI, De Lima JLMP, Maltese A, Frances F, Caylor K, Kohv M, Perks M, Ruiz-Pérez G, Su Z, Vico G, Toth B (2018) On the use of unmanned aerial systems for environmental monitoring. Remote Sensing 10:641. https://doi.org/10.3390/rs10040641

Marcaccio JV, Markle CE, Chow-Fraser P (2016) Use of fixed-wing and multi-rotor unmanned aerial vehicles to map dynamic changes in a freshwater marsh. Journal of Unmanned Vehicle Systems 4(3):193–202. https://doi.org/10.1139/juvs-2015-0016@juvs-ic.issue01

Martin S (2015) The coastal Palmetto Bay and Cutler Bay habitat restoration project. https://regionalconservation.org/ircs/NAWCA.pdf Accessed 15 Nov 2019

Maxwell AE, Warner TA, Fang F (2018) Implementation of machine-learning classification in remote sensing: an applied review. International Journal of Remote Sensing 39(9):2784–2817. https://doi.org/10.1080/01431161.2018.1433343

Meng X, Shang N, Zhang X, Li C, Zhao K, Qiu X, Weeks E (2017) Photogrammetric UAV mapping of terrain under dense coastal vegetation: an object-oriented classification ensemble algorithm for classification and terrain correction. Remote Sensing 9(11):1187. https://doi.org/10.3390/rs9111187

Morris JT, Sundareshwar PV, Nietch CT, Kjerve B, Cahoon DR (2002) Responses of coastal wetlands to rising sea level. Ecology 83(10): 2869–2877. https://doi.org/10.1890/0012-9658(2002)083[2869:ROCWTR]2.0.CO;2

Nex F, Remondino F (2014) UAV for 3D mapping applications: a review. Applied Geomatics 6(1):1–15. https://doi.org/10.1007/s12518-013-0120-x

Obanawa H, Sakanoue S, Yagi T (2019) Evaluating the applicability of RTK-UAV for field management. IGARSS 2019–2019 IEEE International Geoscience and Remote Sensing Symposium, Yokohama, pp. 9090–9092. https://doi.org/10.1109/IGARSS.2019.8897895

Pande-Chhetri R, Abd-Elrahman A, Liu T, Morton J, Wilhelm VL (2017) Object-based classification of wetland vegetation using very high-resolution unmanned air system imagery. European Journal of Remote Sensing 50(1):564–576. https://doi.org/10.1080/22797254.2017.1373602

Peppa MV, Hall J, Goodyear J, Mills JP (2019) Photogrammetric assessment and comparison of DJI phantom 4 pro and phantom 4 RTK small unmanned aircraft systems. In International Archives of the Photogrammetry, Remote Sensing and Spatial Information Sciences, XLII-2/W13, 503–509. ISPRS Geospatial Week, Enschede. https://doi.org/10.5194/isprs-archives-XLII-2-W13-503-2019

Pimentel D, Lach L, Zuniga R, Morrison D (2000) Environmental and economic costs of nonindigenous species in the United States. BioScience 50(1):53–65. https://doi.org/10.1641/0006-3568(2000)050[0053:EAECON]2.3.CO;2

Prošek J, Šímová P (2019) UAV for mapping shrubland vegetation: does fusion of spectral and vertical information derived from a single sensor increase the classification accuracy? International Journal of Applied Earth Observation and Geoinformation 75:151–162. https://doi.org/10.1016/j.jag.2018.10.009

Ramirez AHM, Jhala AJ, Singh M (2012) Germination and emergence characteristics of common Beggar's-tick (Bidens Alba). Weed Science 60(3):374–378. https://doi.org/10.1614/WS-D-11-00167.1

Ramsey EW, Jensen JR (1996) Remote sensing of mangrove wetlands: relating canopy spectra to site specific data. Photogrammetric Engineering and Remote Sensing 62(8):939–948

Sharpe JM (2010) Responses of the mangrove fern Acrostichum danaeifolium Langsd. & Fisch. (Pteridaceae, Pteridophyta) to disturbances resulting from increased soil salinity and hurricane Georges at the Jobos Bay National Estuarine Research Reserve, Puerto Rico. Wetlands Ecology and Management 18(1):57–68. https://doi.org/10.1007/s11273-009-9148-4

Strecha C, Fletcher A, Lechner A, Erskine P, Fua P (2012) Developing species specific vegetation maps using multi-spectral hyperspatial imagery from unmanned aerial vehicles. International Archives of the Photogrammetry, Remote Sensing, and Spatial Information Sciences, 1–3, 311–316. XXII ISPRS Congress, Melbourne

Tomlinson PB (2016) The botany of mangroves, 2nd edn. Cambridge University Press, Cambridge (Chapter 5)

Trimble (2014) eCognition developer 9.0.1 reference book. Trimble Germany GmnH, Munich

U.S. Fish and Wildlife Service. Species status assessment: Monarch butterfly (2018) https://www.fws.gov/savethemonarch/pdfs/MonarchSSAFactSheet.pdf Accessed 3 March 2020

UF IFAS. Saltbush-a native beauty, of sorts (2016) http://blogs.ifas.ufl.edu/escambiaco/2016/09/16/saltbush-a-native-beauty-of-sorts/ Accessed 3 March 2020

US Army Corps of Engineers. National Wetland Plant List. (2018) http://wetland-plants.usace.army.mil/nwpl_static/v33/home/home.html Accessed 3 March 2020

Vapnik V (1995) The nature of statistical learning theory. Springer-Verlag, New York. https://doi.org/10.1007/978-1-4757-2440-0

Wilcove DS, Rothstein D, Dubow J, Phillips A, Losos E (1998) Quantifying threats to imperiled species in the United States. BioScience 48(8):607–615. https://doi.org/10.2307/1313420

Zhang C, Xie Z (2013) Object-based vegetation mapping in the Kissimmee River watershed using HyMap data and machine learning techniques. Wetlands 33(2):233–244

Zhang C, Selch D, Cooper H (2016) A framework to combine three remotely sensed data sources for vegetation mapping in the Central Florida Everglades. Wetlands 36(2):201–213. https://doi.org/10.1007/s13157-015-0730-7

Zhang C, Denka S, Mishra DR (2018) Mapping freshwater marsh species in the wetlands of Lake Okeechobee using very high-resolution aerial photography and lidar data. International Journal of Remote Sensing 39(17):5600–5618. https://doi.org/10.1080/01431161.2018.1455242

Zhao Q, Bai J, Huang L, Gu B, Lu Q, Gao Z (2016) A review of methodologies and success indicators for coastal wetland restoration. Ecological Indicators 60:442–452. https://doi.org/10.1016/j.ecolind.2015.07.003

Zweig CL, Burgess MA, Percival HF, Kitchens WM (2015) Use of unmanned aircraft systems to delineate fine-scale wetland vegetation communities. Wetlands 35(2):303–309. https://doi.org/10.1007/s13157-014-0612-4